Spin-Josephson effects in exchange coupled antiferromagnetic insulators

Yizhou Liu, Gen Yin, Jiadong Zang, Roger K. Lake, and Yafis Barlas

Phys. Rev. B **94**, 094434 — Published 26 September 2016

DOI: 10.1103/PhysRevB.94.094434

Spin Josephson effects in Exchange coupled Antiferromagnetic Insulators

Yizhou Liu,[1,2] Gen Yin,[1,2] Jiadong Zang,[3] Roger K. Lake,[1,2,*] and Yafis Barlas[2,4,†]

[1] *Department of Electrical and Computer Engineering, University of California, Riverside, CA 92521, USA*
[2] *Center of Spins and Heat in Nanoscale Electronic Systems, University of California, Riverside, CA 92521, USA*
[3] *Department of Physics and Materials Science Program, University of New Hampshire, Durham, New Hampshire 03824, USA*
[4] *Department of Physics and Astronomy, University of California, Riverside, CA 92521, USA*

The spin superfluid analogy can be extended to include Josephson-like oscillations of the spin current. In a system of two antiferromagnetic insulators (AFMIs) separated by a thin metallic spacer, a threshold spin chemical potential established perpendicular to the direction of the Néel vector field drives terahertz oscillations of the spin current. This spin current also has a non-linear, time-averaged component which provides a 'smoking gun' signature of spin superfluidity. The time-averaged spin current can be detected via the inverse spin Hall effect in a metallic spacer with large spin-orbit coupling. The physics illustrated here with AFMIs also applies to easy-plane ferromagnetic insulators. These findings may provide a new approach for experimental verification of spin superfluidity and realization of a terahertz spin oscillator.

I. INTRODUCTION

One main objective in the field of spintronics is the generation and manipulation of pure spin currents in magnetically ordered systems. Pure spin currents in magnetic insulators are carried by collective excitations. This can be achieved by combining elements of conventional spintronics with magnetic insulators [1], for example, magnon mediated spin currents can be generated in heterostructures composed of ferromagnetic(FM) insulators and metals [2, 3]. A more exotic method of transporting spin harnesses the ground states of both easy-plane FMs [4–6] and antiferromagnetic insulators (AFMIs) [7]. It has been long appreciated that magnetically ordered systems with spontaneously broken $U(1)$ symmetry [8, 9] support metastable spin spiral states that can transfer spin angular momentum without dissipation [10]. In this regard, heterostructures composed of AFMIs are advantageous to those composed of easy-plane FMs, since they are less sensitive to stray fields or dipolar interactions, which can destroy dissipationless spin transport in easy-plane FMs [11].

It is difficult to experimentally distinguish between spin super-currents and magnon mediated spin currents in magnetic insulators, since the spin wave decay length is long due to the small Gilbert damping. Therefore, other signatures of spin superfluidity in magnetically ordered systems need to be explored. To this end, it is advantageous to investigate the connections between superconductivity and magnetism further. One remarkable phenomena is the Josephson effect [12], which occurs in coupled superfluids and superconductors because the coupling energy is a periodic function of the relative phase difference. A similar energy dependence can be anticipated for exchange coupled AFMIs and easy-plane FMs. This insight suggests that it is instructive to analyze the effect of exchange coupling on the spin currents in heterostructures composed of exchange coupled AFMIs and easy-plane FMs. Josephson dynamics were also predictied in dipole coupled nanomagnets [13].

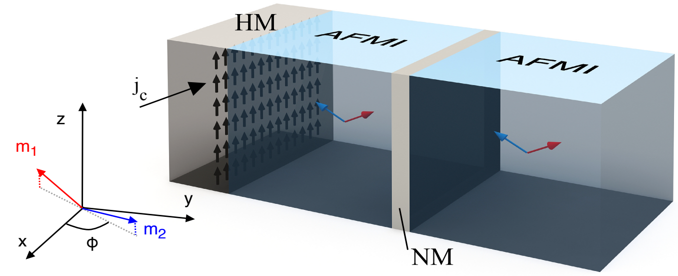

FIG. 1. Schematic diagram of the proposed heterostructure to detect the Josephson effect in spin superfluids. The heterostructure consists of two antiferromagnetic insulators (AFMIs) separated by a thin non-magnetic metallic (NM) spacer. The magnetization of the AFMIs lies in the xy-plane as indicated in the inset showing the direction of the Néel vector and phase ϕ, with a spin canting in the $\hat{z}$-direction. A spin chemical potential of up spins on the left interface of the AFMI can drive an oscillating spin current through the metallic spacer via spin pumping. The spin Hall effect in a heavy metal (HM) can inject a spin current. The spin current flowing through a spin-orbit (SO) coupled metallic spacer can be detected via the inverse spin Hall effect.

In this article, we propose a lateral spin valve heterostructure, which consists of two AFMIs separated by a thin metallic spacer [14]. We show that the spin superfluid analogy can be further extended to realize Josephson-like oscillations of the spin currents flowing through exchange coupled antiferromagnetic insulators (AFMIs). This oscillatory spin current can be detected

* Corresponding author: rlake@ece.ucr.edu
† Corresponding author: yafisb@ucr.edu

by injecting a pure spin current on the left side of the heterostructure illustrated in Fig. 1. A spin chemical potential established perpendicular to the direction of the Néel vector field, drives an oscillatory spin supercurrent which can be converted to a charge current via the inverse spin Hall effect through a metallic spacer with large spin-orbit coupling. Furthermore, this oscillatory spin current induces a non-Ohmic I_S-V_S characteristics of AFMI exchange coupled heterostructures, which provides a "smoking gun" signature of the spin superfluidity.

II. COUPLED MAGNETIZATION DYNAMICS

Consider the heterostructure in Fig. 1, consisting of two bipartite lattice AFMIs separated by a thin non-magnetic metallic spacer that provides a local interlayer exchange coupling between the two AFMIs. Each AFMI has a staggered spin orientation $\mathbf{s}_i(\mathbf{r}) = S_i(\mathbf{r})/S$ where $i = \pm$ denotes the left (right) AFMI and S is the saturated spin density. The long-wavelength effective Hamiltonian describing the fluctuation of the AFMIs can be expressed in terms of two continuum fields $\mathbf{n}_i(\mathbf{r})$ (the Néel vector field) and $\mathbf{m}_i(\mathbf{r})$ (the canting field), with the local spin orientation $\mathbf{s}_i(\mathbf{r}) = \eta_{i,\mathbf{r}}\mathbf{n}_i(\mathbf{r})\sqrt{1-|\mathbf{m}_i(\mathbf{r})|^2} + \mathbf{m}_i(\mathbf{r})$ with the constraints $|\mathbf{n}_i| = 1$ and $\mathbf{n}_i \cdot \mathbf{m}_i = 0$, where $\eta_{i,\mathbf{r}} = \pm 1$ for the $A(B)$ sublattices [15]. Assuming that the Néel vectors lie in the xy-plane with an interlayer exchange interaction $\sum_{\mathbf{r},\mathbf{r}'} J_{\mathbf{r},\mathbf{r}'}\mathbf{s}_{L,\mathbf{r}} \cdot \mathbf{s}_{R,\mathbf{r}'}$ [16], the effective Hamiltonian capturing the long-wavelength dynamics of this system is,

$$\mathcal{H} = \frac{1}{\mathcal{V}}\int d\mathbf{r}\sum_{i=\pm 1}\left[\frac{\rho}{2}\big(\nabla\mathbf{n}_i(\mathbf{r})\big)^2 + \frac{\lambda}{2}\mathbf{m}_i^2(\mathbf{r}) + \frac{J}{2}\mathbf{n}_i(\mathbf{r})\cdot\mathbf{n}_{-i}(\mathbf{r}) + \frac{J}{2}\mathbf{m}_i(\mathbf{r})\cdot\mathbf{m}_{-i}(\mathbf{r})\right], \tag{1}$$

where $\mathcal{V}$ is the volume, J is the inter-layer exchange coupling of the two AFMIs, $\lambda > 0$ is the homogenous AFMI exchange coupling, and ρ is the spin stiffness assumed equal for both AFMIs [17]. The energy of each AFMI is independent of the direction of the Néel vector $\mathbf{n}_i$ indicating $U(1)$ symmetry, and $\lambda > 0$ ensures that $\mathbf{m}_i = 0$ in equilibrium.

The long wavelength dynamics of the isolated system can be captured by the Landau-Lifshitz-Gilbert(LLG) equations, which subjected to the AFMI constraints, can be expressed as,

$$\hbar\dot{\mathbf{n}}_i = \lambda\mathbf{m}_i \times \mathbf{n}_i + J\mathbf{m}_{-i} \times \mathbf{n}_i - \hbar\alpha\mathbf{n}_i \times \dot{\mathbf{m}}_i, \tag{2}$$

$$\hbar\dot{\mathbf{m}}_i = \rho\mathbf{n}_i \times \nabla^2\mathbf{n}_i + J\mathbf{n}_i \times \mathbf{n}_{-i} - \hbar\alpha\mathbf{n}_i \times \dot{\mathbf{n}}_i, \tag{3}$$

where $(\dot{\mathbf{m}}_i, \dot{\mathbf{n}}_i)$ denote the time derivatives of the fields $(\mathbf{m}_i, \mathbf{n}_i)$, α is the damping constant assumed the same for both AFMIs, and henceforth we neglect the spatial dependence of the fields ($\nabla^2\mathbf{n}_i \sim 0$). To implement the AFM constraints in the above equation we define: $\mathbf{n}_i = (\cos\theta_i\cos\phi_i, \cos\theta_i\sin\phi_i, \sin\theta_i)$, where ϕ is the azimuthal angle, θ is the relative angle to the xy-plane and $\mathbf{m}_i = (-m_{\theta,i}\sin\theta_i\cos\phi_i - m_{\phi,i}\sin\phi_i, -m_{\theta,i}\sin\theta_i\sin\phi_i + m_{\phi,i}\cos\phi_i, m_{\theta,i}\cos\theta_i)$. With these substitutions the long-wavelength dynamics of the coupled AFMIs can be described in terms of a pair of canonically conjugate fields $(m_{\theta,i}, \phi_i)$ and $(m_{\phi,i}, \theta_i)$ for both AFMIs. For small variations about the Néel ordered state $\theta_i \approx 0$, the LLG equations for $(m_{\theta,i}, \phi_i)$ neglecting the quadratic terms, are decoupled from the $(m_{\phi,i}, \theta_i)$ fields, reducing to,

$$\hbar\dot{m}_{\theta,i} = J\sin(\phi_i - \phi_{-i}) - \hbar\alpha\dot{\phi}_i,$$
$$\hbar\dot{\phi}_i = \lambda m_{\theta,i} + Jm_{\theta,-i} + \hbar\alpha\dot{m}_{\theta,i}. \tag{4}$$

For zero damping ($\alpha = 0$), the above equations describing the magnetization dynamics for exchange coupled systems of AFMIs are remarkably similar to the Josephson equations of coupled superconductors. This becomes evident after defining the relative magnetization $m_\theta = m_{\theta,L} - m_{\theta,R}$ and the relative phase $\phi = \phi_L - \phi_R$. Then, Eqs. (4) give

$$\hbar\dot{m}_\theta = 2J\sin(\phi); \quad \hbar\dot{\phi} = (\lambda - J)m_\theta. \tag{5}$$

The time dynamics of the relative phase is governed by $\ddot{\phi} = \omega_0^2\sin(\phi)$, where the characteristic frequency $\omega_0 = \sqrt{2J(\lambda - J)}/\hbar$, depends on the nature of the interlayer exchange of the coupled AFMIs. The equation describing the phase dynamics resembles the equation of a simple pendulum with tilt angle ϕ or equivalently the motion of a particle with unit mass moving in a potential $U(\phi) = \omega_0^2\cos(\phi)$. This mechanical analogue provides an intuitive understanding of the rich magnetization dynamics of Eqs. (4).

Starting with initial conditions $\phi(t = 0) = 0$ and $m_{\theta,0} = 0.05 \propto \dot{\phi}(t = 0)$, we solve Eqs. (4) for both FM and AFM interlayer exchange coupling J. The magnetization exhibits periodic oscillations with frequencies $\omega \sim 1 - 10$ THz, as indicted in Fig. 2, with different dynamics for the FM and AFM inter-layer exchange. Fig. 2(a) shows the periodic variation of the phase dynamics for an FM exchange $|J|/\lambda = 1/300$ with $\lambda = 30meV$, which oscillates about the equilibrium point $\phi = 0$. The magnitude of the oscillations depends on the initial velocity $\dot{\phi}_0 \propto (\lambda - J)m_{\theta,0}/\hbar$. The individual magnetizations ($m_{\theta,L}$ and $m_{\theta,R}$) also exhibits coupled periodic oscillations and as indicated in Fig 2 (b), and the total magnetization is conserved for the isolated system in the absence of any damping. When the initial magnetization is above a critical value $m > m_{0,c} = 2\sqrt{2|J|/(\lambda - J)}$, the Néel vector performs full rotations in the xy-plane, this critical value corresponds to an initial angular velocity of the pendulum $\dot{\phi}_c \geq 2|\omega_0|$. The effect of the Gilbert damping with $\alpha = 0.05$ denoted by the dotted lines in Fig. 2, results in an exponential damping of the phase in time, which in turn, leads to an exponential damping of the total magnetization.

The mechanical analogue for the antiferromagnetic interlayer exchange coupling $J > 0$ corresponds to a simple

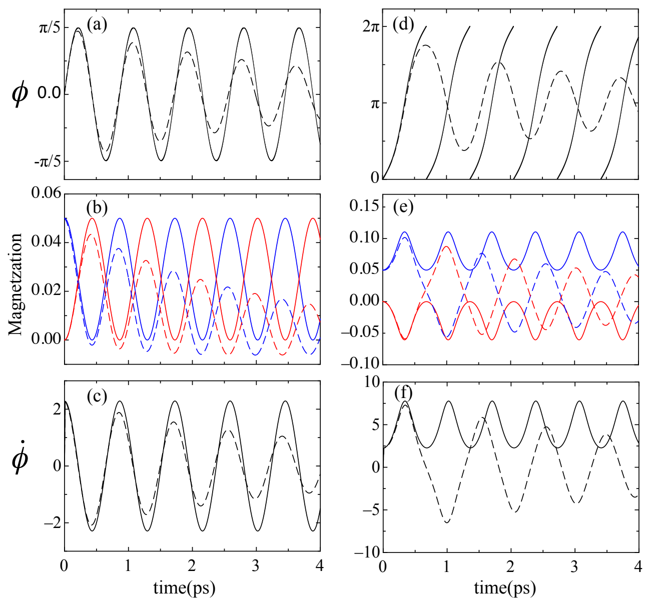

FIG. 2. Dynamics of m_L (blue), m_R (red), ϕ, and the total spin current $I_S/I_{S,0} = \dot{\phi}$ with the initial conditions $m_0 = 0.05$ and $\phi = 0$. (a)-(c) are for the case of a FM inter-layer exchange $J < 0$, and (d)-(f) represent the case for an AFMI inter-layer exchange $J > 0$. All dashed lines represent the dynamics for non-zero damping with $\alpha = 0.05$. The equations are solved for $|J|/\lambda = 1/300$ and $\lambda = 30$ meV.

pendulum with the initial condition $\phi(t = 0) = \pi$, or the π-phase Josephson junction in superconductors. For this case, as shown in Fig. 2(d), irrespective of the initial conditions, the Néel vector performs complete rotations in the xy-plane. $m_{\theta,L}$ and $m_{\theta,R}$ oscillate in-phase leading to an oscillation in m_θ which is conserved in the absence of damping. With damping, ($\alpha = 0.05$), the individual magnetizations decay exponentially as indicated by the dashed lines in Fig. 2, and as before the total magnetization decays exponentially.

III. SPIN-CURRENT DYNAMICS

A. Oscillatory spin-current

The oscillations in the relative magnetization induced by the dynamics in the Néel vector fields of the AFMIs pump a spin current through the metal spacer. This spin current can be written as $I_S = I_{S,L} - I_{S,R}$, where

$$I_{S,i} = \hbar\frac{G_r}{4\pi}(\mathbf{n}_i \times \dot{\mathbf{n}}_i + \mathbf{m}_i \times \dot{\mathbf{m}}_i) - \hbar\frac{G_{im}}{4\pi}(\dot{\mathbf{m}}_i), \tag{6}$$

with $i = L(R)$ and $I_{S,L}(I_{S,R})$ is the spin current injected from the left (right) side of the metallic spacer, $G = \mathcal{A}g^{\uparrow\downarrow}/NS$ is the spin-mixing conductance at the AFMI/spacer interface, $\mathcal{A}$ is the interface area, $g^{\uparrow\downarrow} = g_r^{\uparrow\downarrow} + ig_{im}^{\uparrow\downarrow}$ is the spin-mixing conductance per unit area [18, 19], and $N = \mathcal{V}/a_0^3$ denotes the total number of spins. Restricting to the $\hat{z}$-component of the spin, the spin current pumped into the metallic spacer by the AFMIs can be expressed as,

$$I_S = \hbar\frac{G_r}{4\pi}\dot{\phi}_L - \hbar\frac{G_r}{4\pi}\dot{\phi}_R = \hbar\frac{G_r}{4\pi}\dot{\phi}, \tag{7}$$

valid for $|m_i| \ll |n_i|$. For simplicity, we assume the spin-mixing conductance is real and equal at both AFMI-spacer interfaces.

The normalized $I_S/I_{S,0}$ spin current flowing through metallic spacer, where $I_{S,0} = \hbar G\omega_0/(4\pi)$ is the characteristic spin current supported by the junction, is plotted in Figs. 2(c) and (f) for the FM and the AFM inter-layer exchange. Eq. 7 states that the spin current is proportional to the rate of change of the relative phase, different from the Josephson voltage phase relation in a superconductor. Similarly, we anticipate that the spin chemical potential must act, via spin transfer torque, as a source term for the rate of change of the relative magnetization.

B. Steady state spin-current

Non-equilibrium spin accumulation at the left interface of the first AFMI, via the spin hall effect[20] or anomalous Hall effect, can transfer angular momentum by inducing a spin transfer torque on the coupled AFMI system. The spin-transfer torque can be expressed as

$$\tau_S = \frac{G_r}{4\pi}\mathbf{n} \times \boldsymbol{\mu_S} \times \mathbf{n} + \frac{G_{im}}{4\pi}\boldsymbol{\mu_S} \times \mathbf{n}, \tag{8}$$

where $\boldsymbol{\mu_S} = \boldsymbol{\mu_0} - \hbar\mathbf{n}\times\dot{\mathbf{n}}$ denotes the total non-equilibrium spin accumulation at the left interface, $\boldsymbol{\mu_0}$ is the spin accumulation, and $\hbar\mathbf{n} \times \dot{\mathbf{n}}$ denotes the spin pumping back-action due to the precession of the Néel vector, satisfying Onsager reciprocity [7]. This non-equilibrium spin accumulation leads to a non-zero relative magnetization via spin-transfer torque, resulting in the precession of the Néel vector field that drives an oscillatory spin current through the metallic spacer, which we analyze next.

Consider the spin transfer effect in the $\hat{z}$ spin direction at the left interface and drop G_i. In the presence of a spin accumulation at the left interface, Eq. (3) acquires a spin transfer torque τ_S resulting in modified equations for the canonically conjugate fields $(m_{\theta,i}, \phi_i)$. Eliminating m_θ from the modified equations, the time dynamics of the phase ϕ satisfy,

$$(1+\alpha^2)\ddot{\phi} + \frac{\hbar\tilde{\alpha}\omega^2}{2J}\dot{\phi} - \omega^2\sin(\phi) = \frac{\omega^2}{2J}V_S, \tag{9}$$

where $V_S = G_r^L\mu_0/(4\pi)$, $\tilde{\alpha} = \alpha + \alpha'$ with $\alpha' = G_r/(4\pi)$ is the enhanced damping due to the spin pumping at the spacer, and we define a critical spin voltage $V_{S,c} = 2J$. Here we assume α' is small compared to α and take

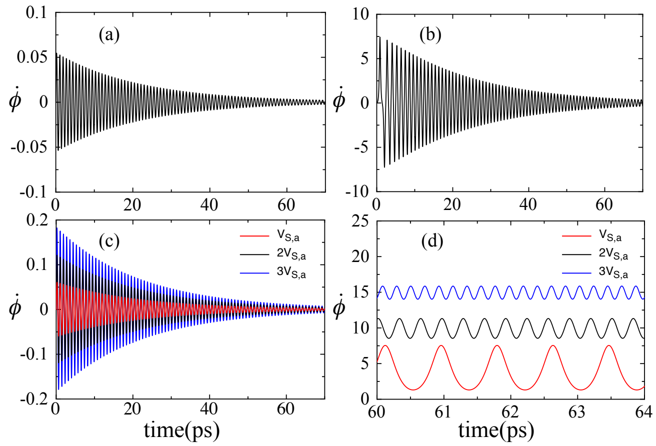

FIG. 3. Steady state solution of $\dot{\phi}$ for the FM inter-layer exchange ($J < 0$) (a, c), and AFM interlayer exchange ($J > 0$) (b, d) as a function of the spin voltage V_S. We choose a spin injection value $V_{S,a} = 0.031J$ that is greater than the critical spin injection. $V_S < V_{S,0}$ for (a) and (b), and $V_{S,a} > V_{S,0}$ for (c) and (d). As before, we set $\lambda = 30meV$, $|J|/\lambda = 1/300$ and $\alpha = 0.001$.

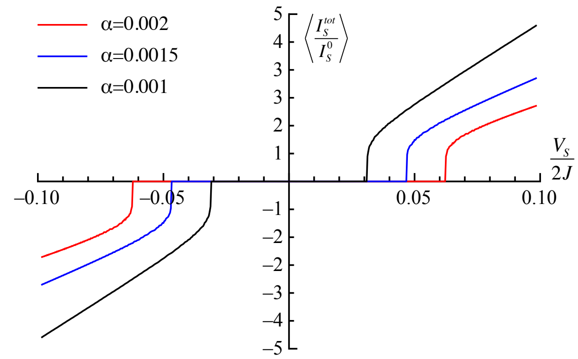

FIG. 4. $I_S - V_S$ characteristics as a function of the applied spin voltage V_S for different values of the damping constant with $\lambda = 30$ meV and $|J|/\lambda = 1/300$.

$\alpha\tilde{\alpha} \sim \alpha^2$. This equation has been extensively studied in the context of superconductivity, and describes the RCSJ model for superconducting Josephson junctions [21]. Based on this similarity, it is prudent to define an effective Stewart-McCumber parameter $\beta = 2J(1+\alpha^2)/(\alpha^2(\lambda - J))$, which determines over-damped ($\beta \ll 1$) or under-damped ($\beta \gg 1$) junctions. For typical values of damping in AFMIs $\beta \sim 2J/(\lambda\alpha^2) \gg 1$, which corresponds to an under-damped junction where Eq. (9) must be solved numerically.

Eq. (9) resembles the equation of motion of a particle of mass $\hbar^2(1+\alpha^2)/(2(\lambda - J))$ moving along the ϕ axis in the presence of an effective tilted washboard potential $U(\phi) = 2J\cos(\phi) - V_S\phi$ with a viscous drag force $\hbar\tilde{\alpha}\dot{\phi}$. The phase dynamics $\dot{\phi}$ in the presence of damping $\alpha = 0.001$ are plotted in Fig. 3 for various values of a constant spin chemical potential V_S. The steady state solution of $\dot{\phi}$ for both the FM or the AFM inter-layer exchange interaction shows the same behavior when $V_S < V_{S,0}$ (see Fig. 3(a) & (b)) and different dynamics when $V_S > V_{S,0}$ (see Fig. 3(c) & (d)), where $V_{S,0} = 0.031J \ll V_{S,c}$ depends on β. When the spin chemical potential is small $V_S < V_{S,0}$, viscous drag dominates the dynamics, and the oscillations in the phase decay as a result of the damping for both the FM and AFM inter-layer exchange interaction. However, if the spin transfer torque induced by V_S is sufficiently large, the energy gain due to the spin transfer torque can balance the energy loss due to the damping resulting in a continual rotation of the Néel vector. In the language of spintronics, this results from the anti-damping like torque due to V_S fully compensating the damping torque. For $J > 0$, which corresponds to the superconducting π-junction, the system is at an unstable equilibrium point, therefore, a small driving force ($V_S \ll 2J$) is enough to induce a full 2π-rotation of the phase. However, for $J < 0$, the system is at an energy minima, so a large driving force $V_S \sim 2J$ is required to overcome both the viscous damping force and the force required to push the particle over the hill.

In the over-damped case $\beta \ll 1$, when $V_S < V_{S,c}$ a static solution for the phase is allowed $\phi = \sin^{-1}(V/(2J))$ implying $I_S = 0$. However, when $V_S > V_{S,c}$ only time dependent solutions exist, for $\beta \ll 1$ we can assume $\langle\ddot{\phi}\rangle \sim 0$, solving Eq. 9 gives an oscillation frequency $\omega = 1/(\hbar\tilde{\alpha})\sqrt{V^2 - 4J^2}$ for the phase ϕ, independent of the sign of the inter-layer exchange interaction. Similar characteristic behavior appears for the case of intermediate damping $\beta \sim 1$, however the critical value of $V_{S,0} = 2\alpha\sqrt{2|J|\lambda}$ to induce a non-zero steady state $\dot{\phi}$, depends on the damping.

IV. I_S-V_S CHARACTERISTICS

The phase dynamics associated with both the FM and AFM inter-layer exchange interactions result in non-Ohmic I_S-V_S characteristics for the AFMI Josephson junctions. The time averaged value for the spin current $I_{S,av}$ can be determined from Eq. (7) for over-damped and under-damped junctions. For over-damped AFMI Josephson junctions $\beta \ll 1$, the $I_S - V_S$ characteristics can be inferred from $I_{S,av} = \hbar G\omega/(4\pi)$ giving the simple relation,

$$I_{S,av} = \frac{G}{4\pi\tilde{\alpha}}\sqrt{V_S^2 - 4J^2} \qquad (10)$$

for $V_S > 2J$, which interpolates smoothly between $I_{S,av} = 0$ and Ohmic behavior with an effective spin resistance $R_S = 4\pi\tilde{\alpha}/G$. The $I_S - V_S$ characteristics for the under-damped junction $\beta \gg 1$ with an AFM inter-layer exchange ($J > 0$) are plotted as function of the spin chemical potential V_S for different values of the damping in Fig. 4. In the under-damped case, the spin current jumps discontinuously from $I_S = 0$ until the spin chemical potential reaches $V_{S,0}$, and $V_{S,0}$ is proportional to β. For under-damped junctions with a FM inter-layer exchange ($J < 0$) $I_{S,av} = 0$ for $V_{S,0} \sim 2J$ where the approximation $|\mathbf{m}| \ll |\mathbf{n}|$ breaks down and requires solutions of LLG equations without any approximations. The $I_S - V_S$ characteristics of AFMI spin Josephson junctions are different from the $I - V$ characteristics of Josephson junctions in superconductors. These differences originate from the spin-current phase relation (see Eq. 7) and the role of the spin transfer torque in exchange coupled AFMIs.

V. DISCUSSION AND SUMMARY

This average spin current flowing between the AFMIs can be detected via the inverse spin Hall effect if the metallic spacer has large spin-orbit coupling [2, 20]. There are several ways to induce a spin chemical potential [6, 7, 11]. Here we consider spin injection by the spin Hall efect. To estimate current densities required to drive a spin current, consider two $0.1\mu\text{m}\times0.1\mu\text{m}\times0.01\mu\text{m}$ NiO thin films, with the exchange energy $\lambda = 19.01\text{meV}$[22]. Taking $\alpha = 0.007$ and $J = 0.1$ meV we find that a spin chemical potential $V_{S,0} = 0.039$ meV is required for a spin current $I_S = 2.2 \times 10^{-2}$ meV. The critical current density can be estimated from the relation $V_S = \hbar G/(4\pi e)\theta_{SH} I_c$. Taking the spin mixing conductance g_r of NiO of $6.9 \times 10^{18}\text{m}^{-2}$ [18], and assuming a 10nm thick Pt spin current injector with $\theta_{SH} \sim 0.1$, we obtain an injection current density $I_c \sim 2.3\times10^7\text{A/cm}^2$. The induced charge current, $I_c = 2e\theta_{SH} I_S/\hbar$ through a thin film Pt spacer with $t = 1$ nm and conductivity ~ 0.095 $(\mu\Omega\text{cm})^{-1}$ gives an induced non-local voltage $V \sim 0.017\mu V$ across the Pt spacer.

The RKKY interaction is one mechanism that can generate the interlayer exchange coupling between the two AFMIs [23]. In this case, the interlayer exchange coupling will be an oscillatory function of $k_F d$ where k_F is the Fermi wavevector and d is the thickness of the non-magnetic metallic spacer. The detailed interlayer exchange coupling for AFMI multilayers will depend on the local spin orientation at the AFMI/non-magnetic metal interface. Exchange coupling between AFMIs has not yet been studied, and it is an important research direction in the emerging field of AFM spintronics.

Similar oscillations in the spin current can occur across exchange coupled easy-plane FMs due to their broken U(1) symmetry. The out-of-plane anisotropy in FMs will play the role of λ in AFMIs and determine the property of the junction. Even in the presence of in-plane anisotropy, we expect these oscillations to persist as long as the spin chemical potential is above the anisotropy energy scale. The higher order LLG terms do not destroy the spin current oscillations, but they do affect their detailed dynamics. Lastly, the spatial variation in the order parameter, neglected here, can nucleate spin solitons or instantons within the junction, which can lead to a Fraunhofer-like interference patterns in the non-local voltage similar to the behavior of critical super-currents in superconducting Josephson junctions.

In summary, we propose a novel effect in exchange coupled AFMIs that is the analogue of the Josephson effect in superfluids. Due to periodic dependence of the exchange energy on the relative phase difference, an oscillatory spin current flows through the metallic spacer that is proportional to the rate of change of the relative inplane orientation of the Néel vector fields. A spin transfer torque induced by a spin chemical potential at one of the interfaces results in non-linear I_S-V_S characteristics that distinguish the proposed lateral spin valve heterostructure composed of AFMIs and provide a signature of spin superfluidity. Furthermore, this heterostructure is an example of a pure spin AFMI terahertz oscillator [24].

ACKNOWLEDGEMENT

This work was supported as part of the Spins and Heat in Nanoscale Electronic Systems (SHINES) an Energy Frontier Research Center funded by the U.S. Department of Energy, Office of Science, Basic Energy Sciences under Award #DE-SC0012670. Initial analytical work was also supported by the NSF ECCS-1408168.

[1] S. S.-L. Zhang and S. Zhang, Phys. Rev. Lett. **109**, 096603 (2012).
[2] Y. Kajiwara, K. Harii, S. Takahashi, J. Ohe, K. Uchida, M. Mizuguchi, H. Umezawa, H. Kawai, K. Ando, K. Takanashi, S. Maekawa, and E. Saitoh, Nature **464**, 262 (2010).
[3] J. Li, Y. Xu, M. Aldosary, C. Tang, Z. Lin, S. Zhang, R. Lake, and J. Shi, Nat. Comm. **7**, 10858 (2016).
[4] J. König, M. C. Bønsager, and A. H. MacDonald, Phys. Rev. Lett. **87**, 187202 (2001).
[5] S. Takei and Y. Tserkovnyak, Phys. Rev. Lett. **112**, 227201 (2014).
[6] H. Chen, A. D. Kent, A. H. MacDonald, and I. Sodemann, Phys. Rev. B **90**, 220401 (2014).
[7] S. Takei, B. I. Halperin, A. Yacoby, and Y. Tserkovnyak, Phys. Rev. B **90**, 094408 (2014).
[8] B. I. Halperin and P. C. Hohenberg, Phys. Rev. **188**, 898 (1969).
[9] E. B. Sonin, Adv. in Phys. **59**, 181 (2010).
[10] Spin supercurrents are analogues of charge or mass supercurrents in superconductors and superfluids. This anal-

ogy is useful even in the absence of strict conservation laws for spin, as long as the violation of the conservation laws is weak.

[11] H. Skarsvåg, C. Holmqvist, and A. Brataas, Phys. Rev. Lett. **115**, 237201 (2015).

[12] B. D. Josephson, Physics Letters **1**, 251 (1962).

[13] S. Borlenghi, S. Iubini, S. Lepri, L. Bergqvist, A. Delin, and J. Fransson, Phys. Rev. E **91**, 040102 (2015).

[14] The same phenomena should be anticipated in similar heterostructures composed of easy-plane FMs.

[15] F. D. M. Haldane, Phys. Rev. Lett. **50**, 1153 (1983).

[16] P. Bruno, Phys. Rev. B **52**, 411 (1995).

[17] A. Auerbach, *Interacting Electrons and Quantum Magnetism*, edited by J. L. Birman, J. W. Lynn, M. P. Silverman, H. E. Stanley, and M. Voloshin, Graduate Texts in Contemporary Physics (Springer New York, New York, NY, 1994).

[18] R. Cheng, J. Xiao, Q. Niu, and A. Brataas, Phys. Rev. Lett. **113**, 057601 (2014).

[19] Y. Tserkovnyak, A. Brataas, and G. E. W. Bauer, Phys. Rev. Lett. **88**, 117601 (2002).

[20] J. Sinova, S. O. Valenzuela, J. Wunderlich, C. Back, and T. Jungwirth, Rev. Mod. Phys. **87**, 1213 (2015).

[21] T. V. Duzer and C. W. Turner, *Principles of Superconductive Devices and Circuits* (Prentice Hall, 1999).

[22] M. T. Hutchings and E. J. Samuelsen, Phys. Rev. B **6**, 3447 (1972).

[23] Y. Yafet, Phys. Rev. B **36**, 3948 (1987).

[24] R. Cheng, D. Xiao, and A. Brataas, Phys. Rev. Lett. **116**, 207603 (2016).